

1 Supplementary Table

In this Table we present the log of the observations, with details on the acquisition, and part of the photometric results. Low-resolution spectra of SN 2006aj have been obtained with the ESO VLT UT1 and UT2 telescopes, equipped with the FOcal Reducer Spectrographs (FORS1 and FORS2), and with the Lick telescope, equipped with the Kast Dual-Beam Spectrograph (KDBS) with the D55 dichroic. A high-resolution spectrum of the source was acquired with the VLT UT2 equipped with UVES. Photometry in the *BVRI* bands has been performed simultaneously with each spectrum with the VLT and with the 0.76 m Katzman Automatic Imaging Telescope (limited to the Lick+KDBS observation), except on March 8, when only *BVR* photometry was acquired³¹. Spectroscopic monitoring was discontinued on 10 March 2006, due to Sun elevation constraints. However, photometry was performed for a few more days with the VLT. In Column 1 we report the observation date, in Column 2 the telescope and instrument used, in Column 3 the observing setup, in Column 4 the exposure times of the spectra, in Column 5 the seeing during the spectrum acquisition, in Column 6 the magnitudes not corrected for the Galactic and intrinsic extinction, nor for the host-galaxy flux contribution, and in Column 7 the same magnitudes reported in Column 6, but corrected for the host-galaxy flux. The associated errors are 1σ uncertainties.

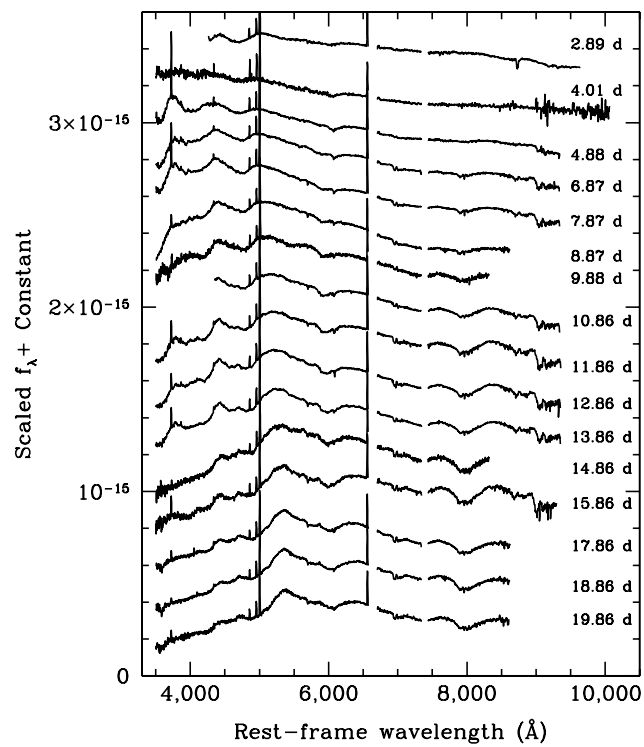
Supplementary Table 1: Summary of observations of SN 2006aj.

Date	Telescope+	Setup	Integr.	Seeing	V	V_{sub}
(2006 UT)	Instrument		Time (s)	(arcsec)	magnitude	magnitude
Feb 21.041	UT1+FORS2	300V+GG435	1800	1.70	18.17 ± 0.03	18.36 ± 0.04
Feb 22.159	Lick+KDBS	D55+600/4310	6000	2.02	17.92 ± 0.08	18.06 ± 0.09
		+300/7500				
Feb 23.026	UT1+FORS2	300V	1800	1.68	17.80 ± 0.03	17.93 ± 0.03
Feb 25.023	UT1+FORS2	300V	1800	1.13	17.58 ± 0.03	17.68 ± 0.03
Feb 26.016	UT1+FORS2	300V	1800	1.08	17.51 ± 0.03	17.61 ± 0.03
Feb 27.023	UT2+FORS1	300V	1800	1.77	17.46 ± 0.03	17.55 ± 0.03
Feb 28.025	UT2+FORS1	300V	2593	1.14	17.45 ± 0.03	17.54 ± 0.03
Mar 01.009	UT1+FORS2	300V+GG435	1800	1.14	17.45 ± 0.03	17.54 ± 0.03
Mar 02.007	UT1+FORS2	300V	1800	1.63	17.47 ± 0.03	17.56 ± 0.03
Mar 03.010	UT1+FORS2	300V	1800	1.12	17.51 ± 0.03	17.61 ± 0.03
Mar 04.009	UT1+FORS2	300V	1800	1.26	17.56 ± 0.03	17.66 ± 0.03
Mar 04.021	UT2+UVES	Dic. 1/390B	2100	1.26		
		+564R				
Mar 05.027	UT2+FORS1	300V	1350	0.83	17.60 ± 0.03	17.71 ± 0.03
Mar 06.014	UT1+FORS2	300V	1800	1.70	17.68 ± 0.03	17.79 ± 0.03
Mar 08.007	UT2+FORS1	300V	1800	1.89	17.86 ± 0.03	18.00 ± 0.03
Mar 09.013	UT2+FORS1	300V	1800	0.95	17.92 ± 0.03	18.06 ± 0.03
Mar 10.013	UT2+FORS1	300V	1560	1.40	18.01 ± 0.03	18.17 ± 0.03

2 Supplementary Figure and Legend

In this Figure we report the VLT FORS1/2 and Lick spectra of SN 2006aj taken at a resolution of 3.4 Å/pixel (FORS1), 2.6 Å/pixel (FORS2), and 1.9/4.6 Å/pixel (Lick, blue and red sides, respectively), reduced to rest frame and scaled up by arbitrary factors for clarity. For each spectrum the time elapsed since XRF 060218 explosion (Feb 18.149, 2006) is indicated, in days. The spectroscopic and photometric data (see Supplementary Table 1) were reduced following standard procedures within the IRAF and MIDAS data reduction packages, respectively. IDL routines were also used for the reduction of the Lick spectrum. Telluric absorption features have been removed. To account for slit losses, the spectra were normalized to the simultaneous V -band photometry: each spectrum was convolved with the response function of the Bessell V filter and the scaling factor was determined by comparison with the V -band measured magnitude. Finally, the contribution of the host-galaxy continuum was subtracted from the spectra and photometry, by linearly interpolating its fluxes^{32–34}. No correction for interstellar reddening was applied to the spectra. Owing to the large airmass at which the observations were performed, the relative flux calibration of the spectra shortward of ~ 4500 Å is not completely reliable. The low-contrast features visible in some VLT spectra longward of ~ 9000 Å are also not meaningful. The spectra show broad absorption lines indicative of high-velocity ejecta, comparable to those present in other energetic Type Ic supernovae³⁵, although not as high as in typical GRB-supernovae^{36–40}. Superimposed on the spectra are emission lines from the host galaxy. Using the $H\alpha$ and [O II] line luminosities we derive⁴¹ a star-formation rate of $\sim 0.06 M_{\odot} \text{ yr}^{-1}$.

Fig. 1.— **Supplementary Figure 1: Spectra of SN 2006aj acquired with the VLT and Lick telescopes.**



3 Supplementary Methods

The rate of low luminosity GRBs and XRFs.

If the low-redshift GRBs are really typical of the global GRB population, then their discovery within the current time and sky coverage must be consistent with the local GRB explosion rate as deduced from the very large BATSE GRB sample. In this section, we study under which conditions low-redshift events can be derived from a luminosity function that is consistent with the $\log N - \log S$ relationship for “classical” cosmological bursts.

All local rate estimates made prior to the discovery of GRB 031203 were derived under the hypothesis that classical bursts greatly exceed a minimum luminosity, L_{\min} , of about $5 \times 10^{49} \text{ erg s}^{-1}$. It was not until the discovery of GRB 031203 that it became clear that the three nearby bursts, 980425, 030329 and 031203, were not consistent with a population of bursts with luminosities greatly exceeding that of GRB 980425 (refs. 42,43). The discovery by *Swift* of the underluminous XRF 060218 slightly after one year of operation gives further credence to this hypothesis. A unified picture can therefore only be achieved by extending down the luminosity function.

The luminosity function used here is based on an extension down to the lowest luminosities consistent with the BATSE cumulative distribution of the number of GRBs as a function of their fluence ($\log N - \log S$), and at the same time gives the correct number of low-redshift events as collected by BATSE, *HETE-II* and *Swift*.

The luminosity function is characterized by a smoothed broken power-law,

$$\Phi(L) = \Phi_0 \left[\left(\frac{L}{L_b} \right)^\alpha + \left(\frac{L}{L_b} \right)^\beta \right]^{-1}, \quad (1)$$

where L is the isotropic equivalent luminosity and does not take into account the effects of collimation. The number of bursts with a peak flux $> P$ is then given by:

$$N(> P) = \int_{L_{\min}}^{L_{\max}} \Phi(L) d \log L \int_0^{z_{\max}(L,P)} \frac{R_{\text{GRB}}(z)}{1+z} \frac{dV(z)}{dz} dz \quad (2)$$

where $dV(z)/dz$ is the comoving volume element, which in a flat Λ CDM universe, is given by

$$\frac{dV}{dz} = \frac{c}{H_0} \frac{D_L^2}{(1+z)^2} \frac{1}{(\Omega_M(1+z)^3 + \Omega_\Lambda)^{1/2}}. \quad (3)$$

That such an analysis will be possible follows from the currently-favored idea that GRBs trace the star formation history of the Universe: $R_{\text{GRB}}(z) = R_{\text{SFR}}(z)$. An analytic formula for the cosmic star formation rate per unit comoving volume is adopted here, as given in ref. 44.

The shape of the luminosity function is constrained here by two different methods. First, similarly to ref. 42 we fit the model to the peak flux distribution observed by BATSE (all 2204 bursts from the GUSBAD catalog) by assuming an average *rest frame* GRB spectrum with a peak energy of 200 ± 50 keV and a low (high) energy photon index of -1 ± 0.5 (-2 ± 0.5). The model predictions are then compared to the redshift and luminosities of GRBs detected by BATSE, *HETE-II* and *Swift*, where the sensitivity curves of all three instruments have been used⁴⁵. The individual constraints are subsequently combined to derive the luminosity function's best-fit parameters.

The major uncertainty in the above method concerns L_{\min} , which we fix to be equal to the luminosity of GRB 980425. By using $L_{\max} = 6 \times 10^{52}$ erg s⁻¹, $L_b = 9 \times 10^{50}$

erg s^{-1} , $\alpha = 0.3$, $\beta = 0.95$ in Equations (1) and (2) above we obtain the best statistical description of the data and a local GRB rate of $110_{-20}^{+180} \text{ Gpc}^{-3}\text{yr}^{-1}$.

The local rate of events that give rise to GRBs is therefore at least one hundred times the rate estimated from the cosmological events only (i.e. those observed by BATSE). Interestingly, we find that a single power-law description for the luminosity function is rejected with fairly high confidence and that an intrinsic break in the luminosity function is indeed required.

Obviously, the above calculation is only sketchy and should be taken as an order of magnitude estimate at present, as the observed redshift distributions are likely to be plagued by severe selection effects. It should, however, improve as more bursts with known redshifts are detected. This estimate is nonetheless consistent with the current rate of low-redshift events and is broadly in agreement with conclusions from earlier statistical studies⁴².

4 Supplementary Notes

We report here the references for the previous Supplementary Section 3.

REFERENCES

31. Ferrero, P. *et al.* The GRB 060218/SN 2006aj event in the context of other Gamma-Ray Burst supernovae. *Astron. Astrophys.* submitted, preprint available at <http://arXiv.org/astro-ph/0605058> (2006).
32. Modjaz, M. *et al.* Early-time photometry and spectroscopy of the fast evolving SN 2006aj associated with GRB 060218. *Astrophys. J.* **645**, L21–L24 (2006).
33. Cool, R.J. *et al.* GRB 060218: SDSS pre-burst observations. *GCN Circ.* 4777 (2006).
34. Hicken, M. *et al.* GRB 060218: refined photometric calibration of comparison stars. *GCN Circ.* 4898 (2006).
35. Foley, R.J. *et al.* Optical photometry and spectroscopy of the SN 1998bw-like type Ic supernova 2002ap. *Publ. Astron. Soc. Pacific* **115**, 1220–1235 (2003).
36. Galama, T. J. *et al.* An unusual supernova in the error box of the γ -ray burst of 25 April 1998. *Nature* **395**, 670–672 (1998).
37. Hjorth, J. *et al.* A very energetic supernova associated with the γ -ray burst of 29 March 2003. *Nature* **423**, 847–850 (2003).
38. Stanek, K.Z. *et al.* Spectroscopic discovery of the supernova 2003dh associated with GRB 030329. *Astrophys. J.* **591**, L17–L20 (2003).
39. Matheson, T. *et al.* Photometry and spectroscopy of GRB 030329 and its associated supernova 2003dh: the first two months. *Astrophys. J.* **599**, 394–407 (2003).

40. Malesani, D. *et al.* SN 2003lw and GRB 031203: a bright supernova for a faint Gamma-Ray Burst. *Astrophys. J.* **609**, L5–L8 (2004).
41. Kennicutt, R.C. Star formation in galaxies along the Hubble sequence. *Annu. Rev. Astron. Astrophys.* **36**, 189–232 (1998).
42. Guetta, D., Perna, R., Stella, L. & Vietri, M. Are all Gamma-Ray Bursts like GRB 980425, GRB 030329, and GRB 031203? *Astrophys. J.* **615**, L73–L76 (2004).
43. Coward, D.M. Simulating a faint gamma-ray burst population. *Mon. Not. R. Astr. Soc.* **360**, L77–L81 (2005).
44. Porciani, C. & Madau, P. On the Association of Gamma-Ray Bursts with Massive Stars: Implications for Number Counts and Lensing Statistics *Astrophys. J.* **548**, 522–531 (2001).
45. Band, D.L. Comparison of the Gamma-Ray Burst Sensitivity of Different Detectors *Astrophys. J.* **588**, 945–951 (2003).